Compartmentalized Expression of c-FLIP in Lung Tissues of Patients with Idiopathic Pulmonary Fibrosis

Seung-Ick Cha[1,2,6*], Steve D. Groshong[2,3*], Stephen K. Frankel[2,3], Ben L. Edelman[1], Gregory P. Cosgrove[2,3], Jennifer L. Terry-Powers[1], Linda K. Remigio[1], Douglas Curran-Everett[5], Kevin K. Brown[2,3], Carlyne D. Cool[2,3], and David W. H. Riches[1,3,4]

[1]Program in Cell Biology, Department of Pediatrics, [2]Interstitial Lung Disease Program, Department of Medicine, and [5]Division of Biostatistics and Bioinformatics, National Jewish Health, Denver, Colorado; [3]Division of Pulmonary Sciences and Critical Care Medicine, Department of Medicine, [4]Department of Immunology, and [5]Department of Biostatistics, Informatics, Physiology and Biophysics, University of Colorado Denver School of Medicine, Denver, Colorado; and [6]Department of Internal Medicine, Kyungpook National University School of Medicine and University Hospital, Daegu, Korea

Increased apoptosis of alveolar epithelial cells and impaired apoptosis of myofibroblasts have been linked to the pathogenesis of idiopathic pulmonary fibrosis/usual interstitial pneumonia (IPF/UIP). Fas, a death receptor of the TNF-receptor superfamily, has been implicated in apoptosis of both cell types, though the mechanisms are poorly understood. The goals of this study were: (*1*) to examine the localization of Fas-associated death-domain-like IL-1β-converting enzyme inhibitory protein (c-FLIP), an NF-κB–dependent regulator of Fas-signaling, in lung tissues from IPF/UIP patients and control subjects; and (*2*) to compare c-FLIP expression with epithelial cell and myofibroblast apoptosis, proliferation, and NF-κB activation. c-FLIP expression was restricted to airway epithelial cells in control lung tissues. In contrast, in patients with IPF/UIP, c-FLIP was also expressed by alveolar epithelial cells in areas of injury and fibrosis, but was absent from myofibroblasts in fibroblastic foci and from alveolar epithelial cells in uninvolved areas of lung tissue. Quantification of apoptosis and proliferation revealed an absence of apoptotic or proliferating cells in fibroblastic foci and low levels of apoptosis and proliferation by alveolar epithelial cells. Quantification of NF-κB expression and nuclear translocation revealed strong staining and translocation in alveolar epithelial cells and weak staining and minimal nuclear translocation in myofibroblasts. These findings suggest that: (*1*) c-FLIP expression is induced in the abnormal alveolar epithelium of patients with IPF/UIP, (*2*) the resistance of myofibroblasts to apoptosis in patients with IPF/UIP occurs independently of c-FLIP expression, and (*3*) increased NF-κB activation and c-FLIP expression by the alveolar epithelium may be linked.

Keywords: idiopathic pulmonary fibrosis; c-FLIP; lung, epithelium; myofibroblast

Idiopathic pulmonary fibrosis (IPF) is the most common of the fibrosing idiopathic interstitial pneumonias. Characterized by a chronic, relentless, and usually fatal clinical course, the mean survival after diagnosis is only 2 to 4 years (1). Usual interstitial pneumonia (UIP), a histopathologic pattern characterized by areas of patchy fibrosis, honeycombing, and by the presence of fibroblastic foci (2, 3), is the pathologic pattern associated with IPF. Fibroblastic foci are composed of a network of fibroblasts, α-smooth muscle actin–positive (α-SMA$^+$) myofibroblasts, and newly deposited collagen. These structures are thought to represent the advancing edge of the fibrotic response (4). Although the initiating events in IPF remain poorly understood, injury and apoptosis of type I and type II alveolar epithelial cells are thought to stimulate the proliferation of type II cells to form a cuboidal, hyperplastic alveolar epithelium (5). Some hyperplastic type II cells become apoptotic, especially in areas adjacent to fibroblastic foci (6). In contrast, fibroblasts and myofibroblasts located in fibroblastic foci appear resistant to apoptosis (7, 8). These findings support the view that apoptosis and survival of alveolar epithelial cells and myofibroblasts are independently regulated events, though little is known about the mechanisms governing this differential regulation of apoptosis and cell survival in IPF/UIP.

Fas, a death receptor of the tumor necrosis factor receptor (TNF-R) superfamily, has been implicated in the development of pulmonary fibrosis through its ability to promote injury to, and apoptosis of, alveolar epithelial cells (9, 10). Paradoxically, mice bearing inactivating mutations in Fas (*lpr*) and FasL (*gld*) also spontaneously develop an inflammatory and fibrosing interstitial pneumonia (11). Previous studies have shown that alveolar epithelial cells, fibroblasts, and myofibroblasts express Fas *in vitro* and in the fibrotic lung tissues of patients with IPF/UIP (8). These findings suggest a potential duality in Fas-FasL function in which Fas signaling may initiate epithelial cell apoptosis and contribute to lung injury, but may also promote myofibroblast apoptosis and clearance during the resolution of lung injury. Understanding how these events are regulated may shed new light on the mechanism of lung cell injury, repair, and fibrosis in IPF/UIP.

The mechanisms regulating the induction of apoptosis after Fas ligation have been well characterized. Fas ligation recruits the adaptor protein FADD, which in turn recruits caspase-8 to form the death-inducing signaling complex (DISC) (12). Activated capsase-8 catalyzes the activation of effector caspases 3, 6, and 7, either directly, or indirectly after Bid cleavage and ampli-

CLINICAL RELEVANCE

Differential Fas-mediated apoptosis of alveolar epithelial cells and myofibroblasts is of fundamental importance to the development of idiopathic pulmonary fibrosis (IPF), though how these responses are controlled remains poorly understood. This work will further the understanding of the role of Fas-associated death-domain-like IL-1β-converting enzyme inhibitory protein (c-FLIP) in the regulation of apoptosis in IPF. In addition, induced c-FLIP expression may be an early marker of injury to the alveolar epithelium in patients with IPF.

(*Received in original form October 30, 2008 and in final form February 29, 2009*)

This work was supported by grants HL068628 and HL055549 (D.W.H.R.), and SCOR grant HL67671 (K.K.B. and C.D.C.) from the National Institutes of Health.

* Both authors contributed equally to this work.

Correspondence and requests for reprints should be addressed to David W. H. Riches, Program in Cell Biology, Department of Pediatrics, National Jewish Health, Smith Building, Room A549, 1400 Jackson Street, Denver, CO 80206. E-mail: richesd@njhealth.org

This article has an online supplement, which is accessible from this issue's table of contents at www.atsjournals.org

Am J Respir Cell Mol Biol Vol 42. pp 140–148, 2010
Originally Published in Press as DOI: 10.1165/rcmb.2008-0419OC on April 16, 2009
Internet address: www.atsjournals.org

fication via the mitochondrial death pathway (13). The induction of apoptosis by Fas is inhibited by c-FLIP, an NF-κB–regulated caspase-8 homolog that interacts with Fas-associated FADD to inhibit caspase-8 activation and apoptosis (14). c-FLIP exists as two major isoforms, c-$FLIP_S$ and c-$FLIP_L$, which arise by alternative splicing (15). c-$FLIP_S$, containing the 2 NH_2-terminal death effector domains, serves to inhibit Fas-induced apoptosis (15, 16). c-$FLIP_L$, while capable of inhibiting Fas-induced apoptosis, has additionally been shown to play a role in cell survival through its ability to activate NF-κB and the MEK-ERK signaling pathways after Fas ligation (17, 18). Against this background, the goal of our study was to systematically evaluate the expression and localization of c-FLIP in lung tissues from nondiseased control subjects and from patients with IPF/UIP, with a particular emphasis on the alveolar epithelium and the mesenchymal cells of the fibroblastic foci.

MATERIALS AND METHODS

Study Population

The study population consisted of 10 individuals with surgical lung biopsy–proven UIP and a clinical diagnosis of IPF randomly selected from subjects who had previously been prospectively enrolled in our Human Subjects Institutional Review Board (IRB)-approved Interstitial Lung Disease Program and Specialized Center Of Research (SCOR) protocol at National Jewish Medical and Research Center. Informed consent was obtained from each subject. All patients with IPF/UIP fulfilled the criteria for diagnosis as defined by the consensus classification of the American Thoracic Society and European Respiratory Society (19). Nondiseased whole lung control tissue was obtained from Tissue Transformation Technologies (TTT, Edison, NJ). All individuals suffered brain death and were evaluated for organ transplantation before research consent. In all instances, informed consent was obtained from next-of-kin and/or health care proxy at time of transplantation evaluation. All specimens failed regional lung selection criteria for transplantation. For inclusion, individuals had to have no evidence of active infection, chest radiographic abnormalities, Pa_{O_2}/FI_{O_2} greater than 250, duration of mechanical ventilation less than 48 hours, and no past medical history of underlying lung disease. All samples were received and fixed within 18 hours of procurement. Tables 1 and 2 summarize the demographic and clinical characteristics of patients with IPF/UIP and the demographic data of control subjects, respectively. Subjects were classified as current smokers if they had regularly smoked cigarettes within the previous year, former smokers if they had not smoked cigarettes in the previous year but had smoked before that, and never-smokers.

Clinical Assessment

All subjects underwent a standardized clinical, physiologic, radiographic, and pathologic evaluation. A modified American Thoracic Society (ATS) questionnaire was used to collect demographic and clinical information. The degree of dyspnea was determined by a validated dyspnea scale (20). Disease severity was determined by a modified clinical-radiographic-physiologic (CRP) scoring system (1).

Sample Preparation, Immuno- and TUNEL Staining

Lung tissues were fixed with 10% (vol/vol) formalin and embedded in paraffin. Each block was sequentially cut into 4-μm-thick serial sections on Superfrost/Plus slides (Fisher Scientific, Pittsburgh, PA). All samples were stained with hematoxylin and eosin (H&E) and pentachrome/Movat stain (21) to allow morphometric analysis of fibroblastic tissues, collagen fibers, and elastin. For immunohistochemical staining, tissue sections were deparaffinized in xylene and graded alcohols and subjected to antigen retrieval by heating in citrate buffer, pH 6.0, or by treatment with BORG Decloaker solution (Biocare Medical, Walnut Creek, CA) using a Decloaking Chamber (Biocare Medical). Endogenous peroxidase was blocked by treatment with 3% hydrogen peroxide in deionized water at room temperature for 30 minutes. The tissue distributions of c-FLIP and lineage specific markers were determined by immunohistochemical staining. All antibodies were mouse monoclonal antibodies from Ventana Medical Systems (Tucson, AZ) unless indicated otherwise and were used at a final concentration of 1 to 2 μg/ml. Serial sections were stained with: (*1*) rabbit anti-human c-FLIP antibody reactive with c-$FLIP_L$ and c-$FLIP_S$ (Santa Cruz Biotechnology, Santa Cruz, CA); (*2*) anti-human CD68 (macrophage marker; DAKO, Carpineria, CA); (*3*) anti-human cytokeratin antibody (epithelial cell marker reactive with all cytokeratins except 9, 11, and 12); (*4*) anti-human α-smooth muscle actin antibody (myofibroblast marker); or (*5*) anti-vimentin antibody (fibroblast/myofibroblast marker). Negative controls consisted of nonimmune mouse or rabbit IgG and were used at the same concentration as the primary antibodies. Immunohistochemistry was performed either manually or using an automated immunohistochemical stainer (Ventana ES; Ventana Medical Systems) in which slides were incubated sequentially with each primary or control antibody (30 min, 37°C) followed by biotinylated secondary antibody, avidin-streptavidin-enzyme conjugate, and chromogenic enzyme substrate (4 min, 37°C) according to the manufacturer's protocol (Vectastain ABC kit; Vector Laboratories, Burlingame, CA). This was followed by incubation in copper diaminobenzidine enhancer, hematoxylin counterstaining, and application of a liquid coverslip.

The Dead-End TUNEL assay (Promega, Madison, WI) was used to detect apoptotic cells in lung tissues according to the manufacturer's protocol. Four-micron-thick sections of paraffin-embedded lung tissue on glass slides were deparaffinized using xylene followed by graduated ethanol incubations and then washing in PBS. For the positive control, tissue was incubated in DNase I (5 units/ml in supplied buffer) for 10 minutes at room temperature. Slides were counterstained for 5 minutes in hematoxylin, coverslipped, and photographed using a light microscope equipped with a ×20 objective and digital camera. The percentage of TUNEL-positive cells was assessed by counting 400 cells, either alveolar epithelial cells or stromal cells including fibroblasts and myofibroblasts. Cells showing strong nuclear labeling were considered positive. Neither exfoliated cells in airspaces nor circulating leukocytes in vessels were included in the counts.

TABLE 1. CLINICAL CHARACTERISTICS OF PATIENTS WITH IDIOPATHIC PULMONARY FIBROSIS (*N* = 10)

Case No.	Sex	Age (*yr*)	Smoking Status	FVC (*% pred*)	FEV_1 (*% pred*)	D_{LCO}/V_A (*% pred*)	Resting $P(A\text{-}a)O_2$ (*mm Hg*)	CRP Score
1	M	66	Never-smoker	60	83	70	3	25.7
2	M	75	Former smoker	51	69	120	22	42.7
3	M	77	Former smoker	102	125	36	32	38.0
4	M	64	Never-smoker	96	119	83	14	22.1
5	M	50	Never-smoker	41	46	120	10	36.0
6	F	52	Current smoker	91	79	47	31	32.4
7	F	58	Never-smoker	50	58	81	19	36.1
8	M	67	Former smoker	99	97	41	2	13.0
9	M	53	Former smoker	41	41	90	8	42.6
10	F	65	Never-smoker	44	44	90	99	46.7

Definition of abbreviations: D_{LCO}/V_A, diffusing capacity for carbon monoxide corrected for alveolar volume; FEV_1, forced expiratory volume in one second; FVC, forced vital capacity; $P(A\text{-}a)O_2$, alveolar-arterial partial pressure difference of oxygen.

TABLE 2. DEMOGRAPHIC DATA OF CONTROL SUBJECTS ($N = 9$)

Case No.	Sex	Age	Smoking Status	Causes of Death
1	NA	NA	NA	NA
2	NA	NA	NA	NA
3	M	18	NA	NA
4	M	22	Never-smoker	Head trauma
5	F	17	Never-smoker	Head trauma
6	F	71	Never-smoker	Head trauma
7	F	78	Current smoker	Stroke
8	F	75	Never-smoker	Stroke
9	F	78	Never-smoker	Stroke

Definition of abbreviation: NA, not available.

Morphometric Analysis

A dedicated computer program (KS300 Imaging System; Carl Zeiss, Göttingen, Germany) was used for the morphometric analyses. Digital images were taken using an Axioskop 2 light microscope (Carl Zeiss) equipped with an AxioCam color camera (objective 0.63x; Carl Zeiss). Beginning at the center of each tissue section, 12 consecutive random images were selected with a ×40 objective. After a segmentation procedure, the areas of positive staining were automatically calculated by the computer in a binary image. A ratio of areas was calculated per microscopic field: area of positive staining versus total lung area. This ratio was subsequently multiplied by 100% to yield an area percentage. The 12 images were averaged for each representative section. Ki-67 immunostaining was quantified by counting positive cells per field view.

Transfection and NF-κB Reporter Gene Assay

HEK293 cells were transfected with increasing amounts of a c-FLIP expression construct and constant amounts of NF-κB–luciferase reporter gene (250 ng) and renilla luciferase (100 ng) constructs per well. The total amount of DNA transfected into each well was kept constant using pcDNA3.1. Eighteen hours after transfection, the cells were left unstimulated or were stimulated with hTNF-α (10 ng/ml) as a positive control for 6 hours. The cells were then lysed in passive lysis buffer and a dual luciferase reporter assay was conducted as described by the manufacturer (Promega, Madison, WI) using a Monolight 2010 luminometer. Luciferase activities were normalized to both renillla activity and lysate protein concentration. Equivalent amounts of total lysate protein were subjected to SDS-PAGE and Western blot with an anti–c-FLIP antibody to verify the level of c-FLIP expression in the transfected cells.

Statistical Analysis

The morphometric data were expressed as the mean ± SEM. The Wilcoxon rank-sum test was used to detect any differences in immunoreactivities between patients with IPF and control subjects. The correlation between each variable was assessed with Spearman's correlation coefficient. Two-sided $P < 0.05$ was considered to be statistically significant. For the TUNEL data, a two-sample permutation test compared responses between the IPF and control groups (22). In a permutation test, the resulting P value represents the probability of obtaining a result at least as extreme as the result observed.

RESULTS

Localization of c-FLIP in Nondiseased and Fibrotic Human Lung Tissues

c-FLIP is primarily expressed as two alternatively spliced isoforms, c-FLIP$_L$ and c-FLIP$_S$ (14, 15). To investigate the relative level of expression of both isoforms in human lung tissues, detergent extracts of whole lung tissues from control nondiseased subjects and from patients with IPF/UIP were analyzed by SDS-PAGE and Western blotting with an antibody that recognizes both c-FLIP$_L$ and c-FLIP$_S$. A lysate of HEK293 cells transfected with a plasmid encoding human c-FLIP$_L$ was used as a positive control. Figure E1 in the online supplement shows that c-FLIP$_L$ was detected in both normal and fibrotic lung tissues. Although the amount of c-FLIP$_L$ detected in patients with IPF/UIP trended toward an increase, it was not significant ($P = 0.164$). c-FLIP$_S$ was not detected in lung tissues from control subjects or from patients with IPF/UIP (data not shown).

To investigate the specific localization of c-FLIP in normal human lung tissues, paraffin sections from nine control subjects were immunohistochemically stained for c-FLIP using an antibody that recognizes both c-FLIP$_L$ and c-FLIP$_S$. Figure 1A shows that arterial smooth muscle cells and endothelial cells were negative for c-FLIP staining. In contrast, robust staining was observed in ciliated and nonciliated columnar bronchiolar epithelial cells (Figure 1B). Figure 1C shows that the alveolar

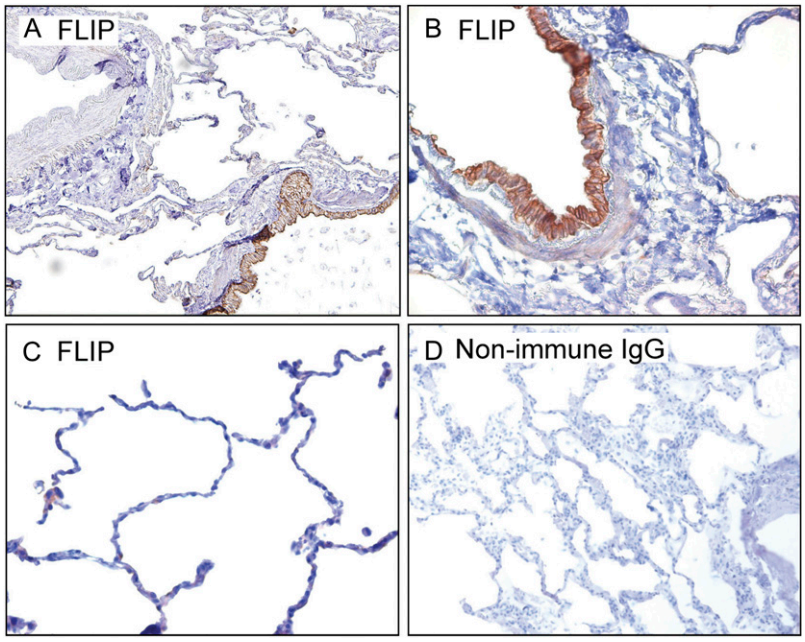

Figure 1. Representative localization of Fas-associated death-domain-like IL-1β-converting enzyme inhibitory protein (c-FLIP) in normal lung tissues. (*A*) c-FLIP is localized to airway epithelial cells (*lower right*) but absent from the cells of the small artery (*upper left*) (×10 objective). (*B*) Higher power micrograph showing strong c-FLIP staining of columnar bronchiolar epithelial cells (×20 objective). (*C*) Low to undetectable staining of c-FLIP in alveolar epithelial cells (×20 objective). (*D*) Control stain with nonimmune IgG and secondary antibody (×4 objective). Sections in *A*–*C* were stained with an antibody that recognizes c-FLIP$_L$ and c-FLIP$_S$.

epithelium of normal lung tissue was largely devoid of c-FLIP staining, although weak staining was occasionally detected in alveolar epithelial cells and alveolar macrophages. As a negative control, background staining was evaluated using a nonimmune IgG in place of the anti–c-FLIP antibody and was found to be negligible (Figure 1D).

Next, we evaluated the localization of c-FLIP in paraffin sections of open lung biopsy specimens from 10 patients with IPF/UIP. As with the nondiseased lung, there was c-FLIP expression in the airway epithelium, but unlike nondiseased parenchymal lung tissues (Figure 1), c-FLIP was expressed by alveolar epithelial cells exhibiting a "hob-nailed" appearance in areas of mild injury associated with modest septal thickening (Figure 2A), and in cuboidal alveolar epithelial cells in areas of greater septal thickening (Figure 2B). There was also extensive c-FLIP staining of the hyperplastic alveolar epithelium overlying fibroblastic foci (Figure 2C). Importantly, in patients with IPF/UIP, c-FLIP staining was not detected in the uninvolved areas of lung parenchyma where the underlying architecture was essentially normal and preserved (Figures 2D–2E). Weak c-FLIP staining was also observed in alveolar macrophages from patients with IPF/UIP, similar to the pattern seen in control nondiseased lung tissues.

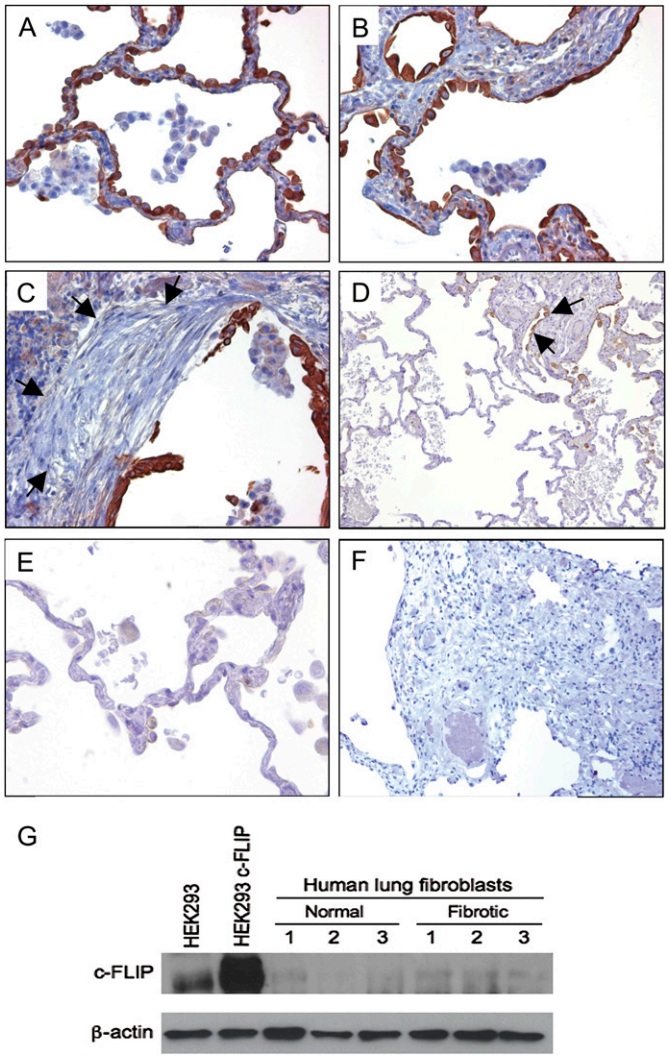

Figure 2. c-FLIP expression in lung tissues from patients with IPF/UIP. (*A–C*) c-FLIP was localized to alveolar epithelial cells including areas of mild injury and septal thickening (*A* and *B*) and cells overlying fibroblastic foci (*C*; *arrows* denote location of fibroblastic focus). c-FLIP was not detected in the mesenchymal cells of the fibroblast foci (*C*). Weak staining was seen in alveolar macrophages (*A–C*). (*D*) Low-power image showing alternating normal and fibrotic lung tissue. Note the absence of c-FLIP staining in areas of normal lung tissue, and positive c-FLIP staining in epithelial cells in a fibrotic area (denoted by *arrows*). (*E*) High-power image showing the lack of c-FLIP staining in a normal area of lung tissue in a patient with IPF/UIP. (*F*) Control stain with nonimmune IgG and secondary antibody (*A*, *B*, *C*, and *E*: ×20 objective; *D* and *E*: ×4 objective). (*G*) Immunoblot for c-FLIP showing low to undetectable expression of c-FLIP in lysates from primary fibroblasts isolated from lung tissues of nondiseased subjects and patients with IPF/UIP. HEK293 cells and HEK293 cells transfected with a c-FLIP expression construct were used as positive controls. An immunoblot for β-actin shows that equal amounts of total protein were loaded onto each lane.

We used morphometric analysis to compare the percentages of c-FLIP–positive cells in lung tissues from patients with IPF/UIP and control subjects without disease. As shown in Figure 3, the percentage of c-FLIP$^+$ lung cells was significantly increased ($P = 0.001$) in IPF/UIP compared with nondiseased control subjects (20.6 ± 2.3% versus 7.9 ± 1.5%, respectively). To confirm the identity of the cell types expressing c-FLIP, serial sections of lung tissues were stained with antibodies against: (*1*) cytokeratin (epithelial cells), (*2*) CD68 (alveolar and interstitial macrophages), and (*3*) α-SMA and vimentin (myofibroblasts/fibroblasts). Figures 4A–4C show that c-FLIP was co-localized primarily with cytokeratin$^+$ alveolar epithelial cells and weakly with CD68$^+$ macrophages. In contrast to the extensive alveolar epithelial staining in patients with IPF/UIP, c-FLIP was not detected in the α-SMA$^+$/vimentin$^+$ myofibroblasts of the fibroblastic foci (Figures 2C and 4D–4F). Furthermore, Western blot analysis of primary cultures of lung fibroblasts from patients with IPF and from nondiseased control subjects revealed low to undetectable expression of c-FLIP (Figure 2G).

NF-κB Activation in Epithelial and Mesenchymal Cells in IPF/UIP

Since the inducible expression of c-FLIP is controlled primarily by the activation of NF-κB (23) and increased expression of c-FLIP was seen in alveolar epithelial cells, but not in fibroblasts or myofibroblasts located in fibroblastic foci of patients with IPF/UIP, we next evaluated the level of NF-κB expression and nuclear translocation of NF-κB by immunohistochemical staining of paraffin sections of lung tissues from normal control subjects and from patients with IPF/UIP. Both normal (Figure 5E) and fibrotic lung tissues (Figures 5A and 5B) were characterized by comparatively stronger staining of NF-κB in alveolar epithelial cells than in other parenchymal cell types. We also detected strong NF-κB staining in small lymphocytes within lymphoid aggregates and regions of septal lymphocytic inflam-

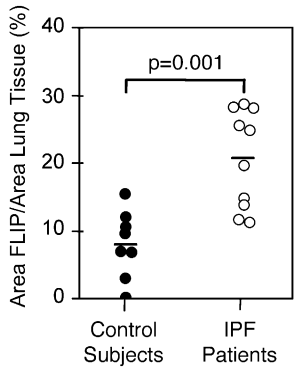

Figure 3. Morphometric analysis of FLIP expression in lung tissues of 10 patients with IPF/UIP and 8 nondiseased control subjects.

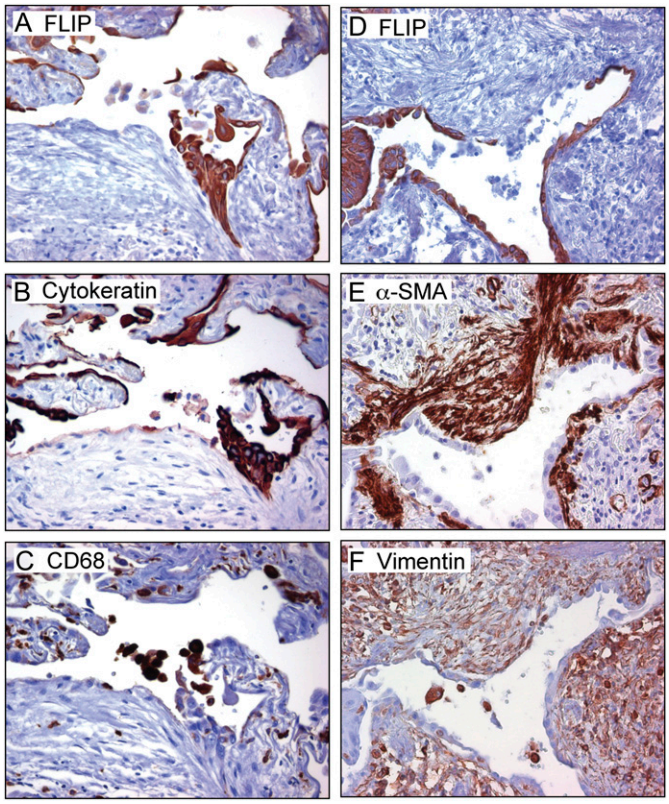

Figure 4. c-FLIP is localized to alveolar epithelial cells, but is absent from myofibroblasts and fibroblasts located in fibroblastic foci in patients with IPF/UIP. (*A–C*) Serial section from a single block stained for (*A*) c-FLIP, (*B*) cytokeratin, and (*C*) CD68. (*D–F*) Serial section from a single block stained for (*D*) c-FLIP, (*E*) α-smooth muscle actin, and (*F*) vimentin (×20 objective for all micrographs).

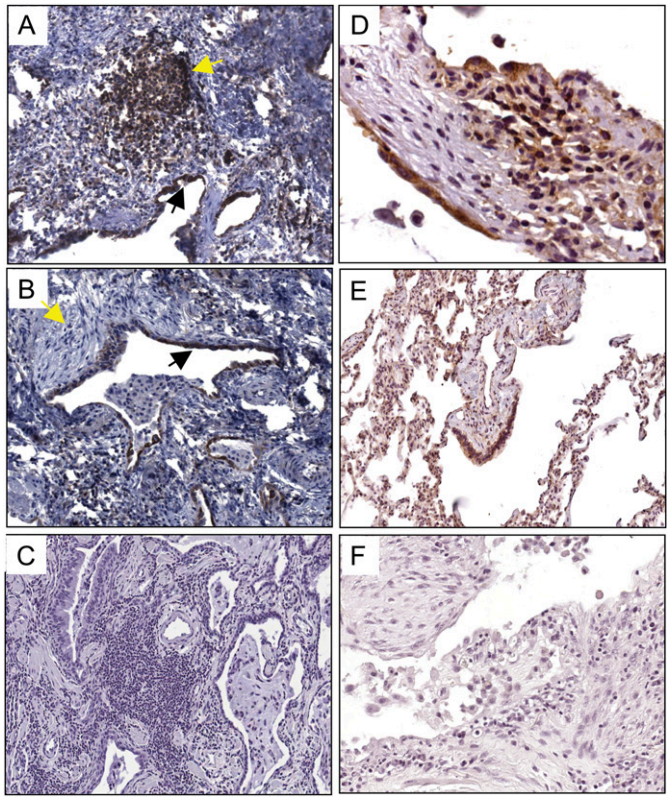

Figure 5. NF-κB expression and nuclear translocation in lung tissues of patients with IPF/UIP and nondiseased control subjects. (*A* and *B*) Low magnification images of lung tissues from patients with IPF/UIP stained for NF-κB showing strong staining by alveolar epithelium (*black arrows* in *A* and *B*) and lymphoid aggregates (*yellow arrow* in *A*). Weak staining of NF-κB is seen in fibroblastic foci (*yellow arrow* in *B*). *A* and *B*: ×10 objective. (*C*) Negative control staining with nonimmune IgG (×4 objective). (*D*) High magnification image of IPF/UIP lung tissue showing strong expression of NF-κB and nuclear translocation in alveolar epithelial cells, and occasional nuclear translocation in fibroblastic cells with a fibroblastic focus (×20 objective). (*E*) Low magnification image of normal lung tissue (×4 objective). (*F*) Negative control staining with nonimmune IgG (×20 objective). Images in *D–F* were incubated in diaminobenzene to increase the sensitivity of detection of NF-κB in mesenchymal cells and were only briefly counterstained in hematoxylin.

mation in sections from IPF/UIP tissues (highlighted by *yellow arrow*, Figure 5A). As expected, normal lung tissue had little lymphocytic inflammation and few lymphoid aggregates. At higher magnification (Figure 5D), focal nuclear translocation of NF-κB was evident in some alveolar epithelial cells and in lymphocytes located in the thickened interstitium. These findings are consistent with the conclusion that increased NF-κB activation in the alveolar epithelium in patients with IPF/UIP may contribute to increased c-FLIP expression.

We also investigated the hypothesis that increased c-FLIP expression might also augment NF-κB activation leading to positive amplification of NF-κB activation. To address this hypothesis, HEK293 cells were co-transfected with increasing amounts of a c-FLIP expression construct and an NF-κB–dependent luciferase reporter gene. Figure E2 shows that increasing c-FLIP expression resulted in a dose-dependent increase in NF-κB activation. These findings suggest that NF-κB–dependent c-FLIP expression may also promote increased NF-κB activation, which in turn leads to a feed-forward amplification cycle to increase c-FLIP expression and further NF-κB activation in the alveolar epithelium of patients with IPF/UIP.

In contrast to the increased staining and nuclear translocation of NF-κB in alveolar epithelial cells in patients with IPF-UIP, only weak NF-κB staining was detected in fibroblasts and myofibroblasts in fibroblastic foci (Figure 5B, *yellow arrow*), even after extended incubation to increase the sensitivity of detection (Figure 5D). Furthermore, nuclear translocation of NF-κB was only occasionally detected in fibroblasts and myofibroblasts in fibroblastic foci (Figure 5D). Quantification of nuclear staining of NF-κB in lung tissues from patients with IPF/UIP revealed nuclear translocation in 21.3 ± 4.4% of alveolar epithelial cells, but only 6.3 ± 2.4% of fibroblasts and myofibroblasts. Nuclear translocation of NF-κB was detected in 10.3 ± 3.1% of alveolar epithelial cells in normal lung tissues.

Apoptosis and Proliferation of Lung Cells in IPF/UIP

The pathogenesis of IPF is thought to involve injury to alveolar epithelial cells, leading to exposure of, and damage to, the alveolar basement membranes. Subsequently, alveolar type II epithelial cells and/or bronchoalveolar stem cells proliferate and attempt to re-epithelialize the exposed or damaged basement membranes, while mesenchymal cells and fibrocytes migrate into the provisional matrix in response to chemotactic cues, including fibronectin, chemokines, and lysophosphatidic acid. Thus, the fibrotic response is thought to involve both injury to epithelial cells and a concomitant accumulation of mesenchymal

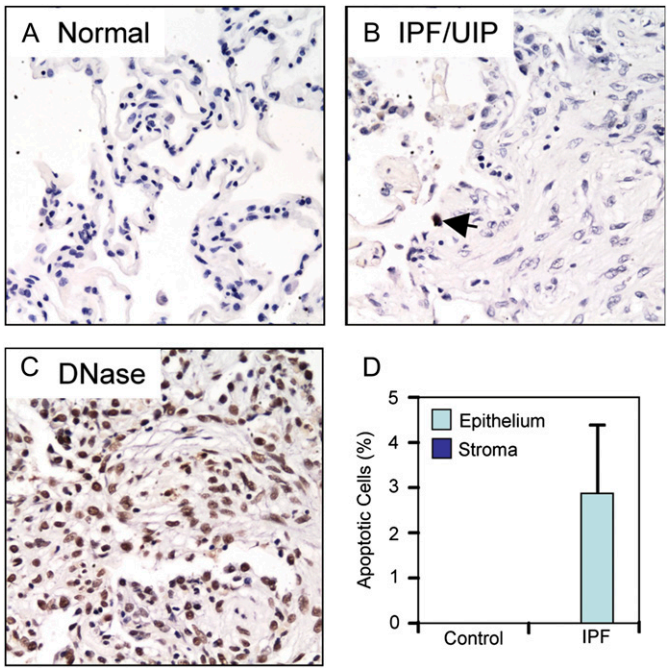

Figure 6. TUNEL staining of apoptotic cells in lung tissues from control subjects and patients with IPF/UIP. (*A*) Normal lung. (*B*) IPF/UIP lung tissue. The *arrow* indicates a single apoptotic alveolar epithelial cell overlying an area of fibrosis. (*C*) DNase-treated lung tissues used as a positive control for TUNEL staining. (*D*) Quantification of the percentage of TUNEL-positive epithelial cells or stromal cells (including fibroblasts and myofibroblasts) in normal lung tissue from control subjects or tissue obtained from patients with IPF/UIP. All micrographs were acquired with a ×20 objective.

cells. To evaluate possible connections between c-FLIP expression and cell injury and apoptosis in lung tissues in patients with IPF/UIP, we quantified the number of apoptotic epithelial and mesenchymal cells by TUNEL staining of normal and IPF/UIP lung tissues. Brief digestion of lung tissues with DNase I was used as a positive control for the TUNEL stain (Figure 6C). Lung tissues from control nondiseased subjects revealed an absence of TUNEL$^+$ cells in both the alveolar epithelium and the few mesenchymal cells found in stromal tissue (Figures 6A and 6D). Lung tissues from patients with IPF/UIP showed a small (2.8 ± 1.5%) but significant ($P = 0.03$) increase in TUNEL$^+$ cells that was restricted exclusively to the alveolar epithelium overlying areas of fibrosis (Figures 6B and 6D). In addition, TUNEL$^+$ cells were not detected within the stromal fibroblastic tissues including the fibroblastic foci, or in areas of lung tissue not involved by fibrosis (Figures 6B and 6D).

Since a small increase in TUNEL$^+$ cells was seen in alveolar epithelial cells in lung tissues from patients with IPF/UIP, we next determined whether there is also an increase in proliferation of epithelial cells that may contribute to epithelial repair. Sections of lung tissues from patients with IPF/UIP were stained for Ki-67, a marker of proliferating cells (24). Figure 7 and Table 3 illustrate the morphologic and morphometric analysis of Ki-67 expression in lung tissues from control subjects and from patients with IPF/UIP. As shown in Figures 7A and 7B, Ki-67 staining was limited to alveolar and columnar airway epithelial cells in nondiseased lung tissues. Ki-67 staining was similarly distributed in lung tissues from patients with IPF/UIP, although a few interstitial cells (mainly lymphocytes) also exhibited Ki-67 staining (Figure 7C). However, Ki-67$^+$ epithelial cells were also detected in areas of epithelial hyperplasia in patients with IPF/UIP (Figure 7D). The percentage of Ki-67$^+$ expressing cells in lung tissues from patients with IPF/UIP (19.8 ± 2.8%) was not significantly different compared with nondiseased lung tissues (11.3 ± 3.2%) (Table 3, $P = 0.08$). Interestingly, Ki-67$^+$ fibroblasts and myofibroblasts were only rarely detected in patients with IPF/UIP. Evaluation of c-FLIP expression in serial sections did not suggest any relationship between the expression of Ki-67 and c-FLIP expression (data not shown).

Relationship between c-FLIP, Collagen, and Elastin Fibers in IPF/UIP

To evaluate the relationship between c-FLIP expression and fibrosis, we conducted morphometric analyses on pentachrome/

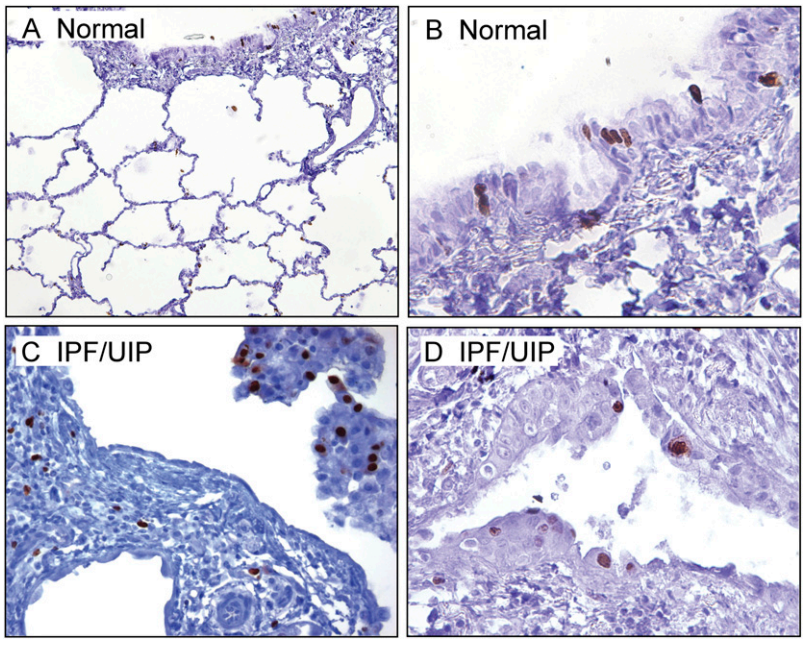

Figure 7. Ki-67 staining in serial sections of lung tissues in IPF/UIP. (*A*) Low magnification of Ki-67 staining indicating sparse staining of alveolar epithelial cells and columnar epithelial cells of airway walls (×10 objective). (*B*) High magnification image a section of a small airway showing Ki-67$^+$ columnar epithelial cells (×40 objective). (*C* and *D*) High magnification images of Ki-67+ alveolar epithelial cells in lung tissues from patients with IPF/UIP. Note the paucity of Ki-67 staining in the fibroblastic focus (centrally located) in *C* and the abundant staining in a region of alveolar epithelial cell hyperplasia (*D*). *C*: ×20 objective; *D*: ×40 objective.

TABLE 3. MORPHOMETRIC ANALYSIS OF EPITHELIAL, MYOFIBROBLAST, MACROPHAGE, AND PROLIFERATION MARKERS IN HUMAN NONDISEASED AND IPF/UIP LUNG TISSUES

	IPF/UIP ($n = 10$)	Nondiseased Control Subjects ($n = 9$)	*P* Value
Cytokeratin (%)	15.0 ± 1.2	48.7 ± 3.2	<0.001
CD68 (%)	16.4 ± 2.5	2.7 ± 0.5	<0.001
Interstitial CD68 (%)	3.7 ± 0.5	1.0 ± 0.3	0.001
α-smooth muscle actin (%)	10.2 ± 3.4	1.4 ± 0.2	<0.001
Vimentin (%)	23.3 ± 1.6	10.9 ± 1.3	<0.001
Ki-67 (cells/field)	19.8 ± 2.8	11.3 ± 3.2	0.08

Definition of abbreviations: IPF, idiopathic pulmonary fibrosis; UIP, usual interstitial pneumonia.

Comparisons were done using the Wilcoxon rank-sum test.

Movat-stained sections of nondiseased and IPF/UIP human lung tissues and quantified the percentages of collagen and elastin fibers. As expected, morphometric analysis revealed that both the amount of collagen and elastin fibers was significantly increased in patients with IPF/UIP compared with nondiseased control subjects (13.0 ± 1.4% versus 1.9 ± 0.5%, $P < 0.001$; and 8.2 ± 1.3% and 2.7 ± 0.4%, $P < 0.001$, respectively). Further, the percentage of total lung c-FLIP expression was significantly correlated with that of collagen fibers ($r^2 = 0.49$, $P = 0.001$), and modestly with that of elastin fibers ($r^2 = 0.30$, $P = 0.016$) (Figures E3A and E3B). Also, as expected, the percentage of α-smooth muscle actin$^+$ cells in lung tissues from patients with IPF/UIP was significantly higher than in nondiseased control lungs (10.2 ± 3.4% versus 1.4 ± 0.2%, $P < 0.001$) (Table 3). However, no significant correlations were observed between total c-FLIP expression and clinical, radiographic, and physiologic factors, including dyspnea, chest radiograph, FEV_1 (% pred), FVC (% pred), D_{LCO}/V_A (% pred), $P(A\text{-}a)O_2$, and CRP score.

DISCUSSION

The mechanisms underlying the pathogenesis of IPF remain incompletely understood, though ongoing injury, apoptosis of alveolar epithelial cells, and accumulation of collagen-producing myofibroblasts in fibroblastic foci are thought to be of central importance (2). Fas, a death receptor of the TNF-R superfamily, has been shown to promote the apoptosis of normal alveolar epithelial cells (25–27), while impaired Fas signaling has been implicated in fibroblast and myofibroblast accumulation in IPF/UIP and in fibroproliferative disorders of the liver and skin (28–30). The mechanisms underlying the differences in susceptibility of lung cells to Fas-mediated apoptosis in IPF/UIP are not fully understood. Here, we show that the expression of c-FLIP, an inducible endogenous inhibitor of Fas-mediated apoptosis, is increased in the lung tissues of patients with IPF/UIP compared with nondiseased control subjects. Lung tissues from normal control subjects exhibited basal expression of c-FLIP by ciliated and nonciliated columnar and pseudostratified airway epithelium, but low to undetectable c-FLIP expression in alveolar epithelium. Consistent with previous animal studies (27, 31), our findings in humans suggest a mechanism that may account for the basal protection of airway epithelial cells from Fas-induced apoptosis, and the exquisite sensitivity of normal alveolar epithelial cells to Fas-induced apoptosis.

In contrast to normal control subjects, c-FLIP was abundantly expressed by the hyperplastic alveolar epithelium of patients with IPF/UIP in areas of mild injury and established fibrosis but was not detected in alveolar epithelial cells in areas of uninvolved lung. Interestingly, increased numbers of CD68$^+$ macrophages were often seen in the alveoli in areas of mild injury and septal thickening adjacent to areas in which c-FLIP was expressed by the alveolar epithelium (D. W. H. Riches, unpublished observations). Thus, it is possible that alveolar macrophages may play a role in the increase in c-FLIP expression by the alveolar epithelium through the production of NF-κB–activating cytokines or other molecules. Consistent with this notion, several cytokines and chemokines that are inducibly produced by macrophages have also been shown to increase c-FLIP expression (e.g., IL-6, IL-8, and IL-12 [32–34]). Alternatively, c-FLIP, through its ability to activate NF-κB and other signaling pathways, may contribute to macrophage accumulation (and inflammation in general) via the production of proinflammatory cytokines or chemoattractants. Though beyond the scope of the present study, these questions could be addressed through the development of transgenic mice expressing c-FLIP in the alveolar epithelium and macrophages via lineage-specific promoters.

Rare apoptosis of alveolar epithelial cells, confirmed herein, has previously been reported in patients with IPF/UIP (7), and some studies have suggested a causative role in the pathogenesis of pulmonary fibrosis (6, 35, 36). Apoptotic alveolar epithelial cells are often found in regions immediately adjacent to fibroblastic foci containing α-SMA$^+$ myofibroblasts (6). These findings have led to the proposal that myofibroblasts secrete pro-apoptotic molecules, and recent studies have suggested that angiotensin peptides (37), FasL (38), and hydrogen peroxide (39) may contribute to alveolar epithelial cell apoptosis. Other studies have shown that alveolar epithelial cell apoptosis can be induced by activation of the innate or adaptive immune systems or by environmental or oxidant stressors (40–42). By quantifying apoptotic cells by TUNEL staining, we detected a small but significant increase in alveolar epithelial cell apoptosis in patients with IPF/UIP compared with control subjects. However, the majority (> 97%) of the alveolar epithelium was TUNEL$^-$. On the one hand, these findings might suggest that expression of c-FLIP by the abnormal alveolar epithelium of patients with IPF/UIP may protect the epithelium from further Fas-induced injury and apoptosis. However, cellular responses to Fas ligation are complex, and c-FLIP can influence Fas signaling often in a lineage-specific fashion, adding further to this complexity (43). For example, c-$FLIP_L$ has been shown to form a herteromeric complex with caspase-8 and augment both caspase-8 activation and the apoptosis in T cells (44). Thus, it is also possible that c-FLIP expression by the alveolar epithelium in patients with IPF/UIP could also contribute to the observed increased apoptosis seen in some of these cells.

After initial injury, type II cell hyperplasia promotes the re-epithelialization of exposed alveolar basement membranes and evolving fibrosis, thereby promoting or enhancing the repair process. In view of the finding of increased apoptosis of alveolar epithelial cells, we also determined whether there was a concomitant increase in epithelial cell proliferation, as reflected by Ki-67 nuclear staining. Ki-67 nuclear staining was detected in alveolar epithelial cells. However, in contrast to the uniform expression of c-FLIP by alveolar epithelial cells in involved areas of lung tissue in IPF/UIP, Ki-67 staining was sporadic and primarily restricted to areas of alveolar epithelial cell hyperplasia. Interestingly, analysis of the expression of c-$FLIP_L$ and c-$FLIP_S$ by Western blotting of lysates of lung tissues revealed that c-$FLIP_L$ was exclusively expressed in both normal subjects and in patients with IPF/UIP. Structure–function studies have shown that both isoforms are capable of inhibiting Fas-induced apoptosis (45). However, unlike c-$FLIP_S$, c-$FLIP_L$ is also involved in the activation of cell survival and proliferative responses via

ERK and NF-κB activation (17, 18). Thus, while our findings suggest that expression of c-$FLIP_L$ is not sufficient to promote alveolar epithelial cell proliferation as reflected by Ki-67 staining, it may contribute to cell survival responses and, through a positive feedback cycle, to the observed increased activation of NF-κB in these cells. This possibility is also supported by the findings present herein and by data reported by Hu and coworkers (46) that increased expression of c-FLIP activates NF-κB in a reporter gene assay.

In contrast to the robust expression of c-FLIP by alveolar epithelial cells in patients with IPF/UIP, fibroblasts and myofibroblasts in fibroblastic foci were uniformly negative for c-FLIP expression. These findings differ from the conclusions of Tanaka and colleagues (47), who reported low but detectable expression of c-FLIP by fibroblasts in patients with IPF. However, the study by Tanaka and colleagues (47) did not employ phenotypic markers to distinguish between fibroblasts and macrophages. Interestingly, quantification of nuclear translocation of NF-κB indicated that only a minor fraction ($\sim$ 6%) of mesenchymal cells within fibroblastic foci exhibited evidence of NF-κB activation. Thus, it is plausible that the absence of c-FLIP expression by mesenchymal cells within fibroblastic foci may be related to their low level of NF-κB activation. Furthermore, we speculate that this low level of NF-κB activation may be consequential to: (*1*) an absence (or sub-threshold presence) of appropriate cytokine or other receptor agonists capable of activating NF-κB within fibroblastic foci; and/or (*2*) the presence of inhibitory cytokines or molecules such as TGF-β, which antagonizes NF-κB activation by proinflammatory stimui (48, 49) and is localized to subepithelial areas of fibrosis in IPF (50, 51).

Consistent with studies reported by Lappi-Blanco and colleagues (7), we did not detect $TUNEL^+$ fibroblasts or myofibroblasts within fibroblast foci or other stromal elements, suggesting that the accumulation of mesenchymal cells within these characteristic structures may occur, in part, as a consequence of a failure to undergo apoptosis. Studies in skin have shown that at the completion of wound repair, recruited fibroblasts and myofibroblasts undergo apoptosis and are rapidly cleared from areas of remodeled tissue (52, 53). Similarly, during alveolarization of the developing lung, accumulated septal myofibroblasts undergo apoptosis once alveolarization is complete (54). *In vitro* studies of fibroblasts and myofibroblasts from normal and fibrotic human lung tissues have shown these cells to be basally resistant to the induction of apoptosis by Fas ligation (30, 47). However, incubation with TNF-α renders the cells exquisitely sensitive to subsequent Fas-induced apoptosis (30), suggesting that a conditional sequence of events, involving TNF-α and Fas ligation, can promote apoptosis. Thus, we speculate that the failure of mesenchymal cells to undergo apoptosis in fibroblastic foci is related to a reduced abundance or activity of TNF-α during the fibroproliferative phase of IPF/UIP. Consistent with this notion, basal expression of TNF-α by alveolar macrophages is extremely low and not significantly different in comparisons between patients with IPF/UIP and healthy control subjects (55, 56), while expression of the anti-inflammatory cytokines IL-10 and TGF-β, which serve to inhibit proinflammatory cytokine expression and function, is increased (50, 56). Since the fibroblasts and myofibroblasts of fibroblastic foci were $TUNEL^-$ and c-$FLIP^-$, our findings also suggest that the resistance of these cells to Fas-induced apoptosis is independent of c-FLIP.

In summary, we have shown herein that the expression of c-FLIP in normal human lung tissues is restricted to the airway epithelium. In contrast, c-FLIP is abundantly expressed by the alveolar epithelium in areas of injury and fibrosis in lung tissues in patients with IPF/UIP. c-FLIP was not detected in the mesenchymal cells of fibroblastic foci, or in uninvolved lung tissues, in patients with IPF/UIP. Further, we have shown that the expression pattern of c-FLIP in patients with IPF/UIP coincides with increased expression and nuclear translocation of NF-κB. Based on these findings, we speculate that: (*1*) NF-κB activation and c-FLIP expression by the alveolar epithelium in patients with IPF/UIP may be mutually interactive, and (*2*) the resistance of the mesenchymal cells of the fibroblastic foci to apoptosis does not involve c-FLIP expression.

Conflict of Interest Statement: None of the authors has a financial relationship with a commercial entity that has an interest in the subject of this manuscript.

Acknowledgments: The authors thank Jane Parr and Raj Praheep for outstanding assistance in the immunohistochemical staining, microscopy, and morphometric analysis. The authors are also indebted to Drs. Peter Henson and Elizabeth Redente, National Jewish Health, for constructive input into this work.

References

1. King TE Jr, Tooze JA, Schwarz MI, Brown KR, Cherniack RM. Predicting survival in idiopathic pulmonary fibrosis: scoring system and survival model. *Am J Respir Crit Care Med* 2001;164:1171–1181.
2. Crystal RG, Bitterman PB, Mossman B, Schwarz MI, Sheppard D, Almasy L, Chapman HA, Friedman SL, King TE Jr, Leinwand LA, *et al.* Future research directions in idiopathic pulmonary fibrosis: summary of a National Heart, Lung, and Blood Institute working group. *Am J Respir Crit Care Med* 2002;166:236–246.
3. Katzenstein AL, Myers JL. Idiopathic pulmonary fibrosis: clinical relevance of pathologic classification. *Am J Respir Crit Care Med* 1998;157:1301–1315.
4. Selman M, King TE, Pardo A. Idiopathic pulmonary fibrosis: prevailing and evolving hypotheses about its pathogenesis and implications for therapy. *Ann Intern Med* 2001;134:136–151.
5. Martin TR, Hagimoto N, Nakamura M, Matute-Bello G. Apoptosis and epithelial injury in the lungs. *Proc Am Thorac Soc* 2005;2:214–220.
6. Uhal BD, Joshi I, Hughes WF, Ramos C, Pardo A, Selman M. Alveolar epithelial cell death adjacent to underlying myofibroblasts in advanced fibrotic human lung. *Am J Physiol* 1998;275:L1192–L1199.
7. Lappi-Blanco E, Soini Y, Paakko P. Apoptotic activity is increased in the newly formed fibromyxoid connective tissue in bronchiolitis obliterans organizing pneumonia. *Lung* 1999;177:367–376.
8. Kazufumi M, Sonoko N, Masanori K, Takateru I, Akira O. Expression of bcl-2 protein and APO-1 (Fas antigen) in the lung tissue from patients with idiopathic pulmonary fibrosis. *Microsc Res Tech* 1997;38: 480–487.
9. Hagimoto N, Kuwano K, Nomoto Y, Kunitake R, Hara N. Apoptosis and expression of Fas/Fas ligand pathway in bleomycin-induced pulmonary fibrosis in mice. *Am J Respir Cell Mol Biol* 1997;16: 91–101.
10. Kuwano K, Hagimoto N, Kawasaki M, Yatomi T, Nakamura N, Nagata S, Suda T, Kunitake R, Maeyama T, Miyazaki H, *et al.* Essential roles of the Fas-Fas ligand pathway in the development of pulmonary fibrosis. *J Clin Invest* 1999;104:13–19.
11. Cohen PL, Eisenberg RA. The lpr and gld genes in systemic autoimmunity: life and death in the Fas lane. *Immunol Today* 1992;13: 427–428.
12. Muzio M, Chinnaiyan AM, Kischkel FC, O'Rourke K, Shevchenko A, Ni J, Scaffidi C, Bretz JD, Zhang M, Gentz R, *et al.* FLICE, a novel FADD-homologous ICE/CED-3-like protease, is recruited to the CD95 (Fas/APO-1) death–inducing signaling complex. *Cell* 1996;85: 817–827.
13. Green DR. Apoptotic pathways: paper wraps stone blunts scissors. *Cell* 2000;102:1–4.
14. Tschopp J, Irmler M, Thome M. Inhibition of fas death signals by FLIPs. *Curr Opin Immunol* 1998;10:552–558.
15. Rasper DM, Vaillancourt JP, Hadano S, Houtzager VM, Seiden I, Keen SL, Tawa P, Xanthoudakis S, Nasir J, Martindale D, *et al.* Cell death attenuation by 'Usurpin', a mammalian DED-caspase homologue that precludes caspase-8 recruitment and activation by the CD-95 (Fas, APO-1) receptor complex. *Cell Death Differ* 1998;5:271–288.
16. Thome M, Schneider P, Hofmann K, Fickenscher H, Meinl E, Neipel F, Mattmann C, Burns K, Bodmer JL, Schroter M, *et al.* Viral FLICE-inhibitory proteins (FLIPs) prevent apoptosis induced by death receptors. *Nature* 1997;386:517–521.

17. Kataoka T, Budd RC, Holler N, Thome M, Martinon F, Irmler M, Burns K, Hahne M, Kennedy N, Kovacsovics M, *et al.* The caspase-8 inhibitor FLIP promotes activation of NF-kappaB and Erk signaling pathways. *Curr Biol* 2000;10:640–648.
18. Luschen S, Falk M, Scherer G, Ussat S, Paulsen M, Adam-Klages S. The Fas-associated death domain protein/caspase-8/c-FLIP signaling pathway is involved in TNF-induced activation of ERK. *Exp Cell Res* 2005;310:33–42.
19. American Thoracic Society/European Respiratory Society. American Thoracic Society/European Respiratory Society International Multidisciplinary Consensus Classification of the Idiopathic Interstitial Pneumonias. *Am J Respir Crit Care Med* 2002;162:277–304.
20. Watters LC, King TE, Schwarz MI, Waldron JA, Stanford RE, Cherniack RM. A clinical, radiographic, and physiologic scoring system for the longitudinal assessment of patients with idiopathic pulmonary fibrosis. *Am Rev Respir Dis* 1986;133:97–103.
21. Movat HZ. Demonstration of all connective tissue elements in a single section; pentachrome stains. *AMA Arch Pathol* 1955;60:289–295.
22. Good PI. Permutation tests: a practical guide to resampling methods for testing hypotheses, 2nd ed. New York: Springer-Verlag; 2000.
23. Micheau O, Lens S, Gaide O, Alevizopoulos K, Tschopp J. NF-kappaB signals induce the expression of c-FLIP. *Mol Cell Biol* 2001;21: 5299–5305.
24. Cool CD, Kennedy D, Voelkel NF, Tuder RM. Pathogenesis and evolution of plexiform lesions in pulmonary hypertension associated with scleroderma and human immunodeficiency virus infection. *Hum Pathol* 1997;28:434–442.
25. Fine A, Anderson NL, Rothstein TL, Williams MC, Gochuico BR. Fas expression in pulmonary alveolar type II cells. *Am J Physiol* 1997;273: L64–L71.
26. Hagimoto N, Kuwano K, Miyazaki H, Kunitake R, Fujita M, Kawasaki M, Kaneko Y, Hara N. Induction of apoptosis and pulmonary fibrosis in mice in response to ligation of Fas antigen. *Am J Respir Cell Mol Biol* 1997;17:272–278.
27. Matute-Bello G, Liles WC, Frevert CW, Nakamura M, Ballman K, Vathanaprida C, Kiener PA, Martin TR. Recombinant human Fas ligand induces alveolar epithelial cell apoptosis and lung injury in rabbits. *Am J Physiol Lung Cell Mol Physiol* 2001;281:L328–L335.
28. Costelli P, Aoki P, Zingaro B, Carbo N, Reffo P, Lopez-Soriano FJ, Bonelli G, Argiles JM, Baccino FM. Mice lacking TNFalpha receptors 1 and 2 are resistant to death and fulminant liver injury induced by agonistic anti-Fas antibody. *Cell Death Differ* 2003;10: 997–1004.
29. Chodon T, Sugihara T, Igawa HH, Funayama E, Furukawa H. Keloid-derived fibroblasts are refractory to Fas-mediated apoptosis and neutralization of autocrine transforming growth factor-beta1 can abrogate this resistance. *Am J Pathol* 2000;157:1661–1669.
30. Frankel SK, Cosgrove GP, Cha SI, Cool CD, Wynes MW, Edelman BL, Brown KK, Riches DW. TNF-alpha sensitizes normal and fibrotic human lung fibroblasts to Fas-induced apoptosis. *Am J Respir Cell Mol Biol* 2006;34:293–304.
31. Nakamura M, Matute-Bello G, Liles WC, Hayashi S, Kajikawa O, Lin SM, Frevert CW, Martin TR. Differential response of human lung epithelial cells to fas-induced apoptosis. *Am J Pathol* 2004;164:1949–1958.
32. Kovalovich K, Li W, DeAngelis R, Greenbaum LE, Ciliberto G, Taub R. Interleukin-6 protects against Fas-mediated death by establishing a critical level of anti-apoptotic hepatic proteins FLIP, Bcl-2, and Bcl-xL. *J Biol Chem* 2001;276:26605–26613.
33. Lee SW, Park Y, Yoo JK, Choi SY, Sung YC. Inhibition of TCR-induced CD8 T cell death by IL-12: regulation of Fas ligand and cellular FLIP expression and caspase activation by IL-12. *J Immunol* 2003;170:2456–2460.
34. Wilson C, Wilson T, Johnston PG, Longley DB, Waugh DJ. Interleukin-8 signaling attenuates TRAIL- and chemotherapy-induced apoptosis through transcriptional regulation of c-FLIP in prostate cancer cells. *Mol Cancer Ther* 2008;7:2649–2661.
35. Kuwano K, Kunitake R, Kawasaki M, Nomoto Y, Hagimoto N, Nakanishi Y, Hara N. P21Waf1/Cip1/Sdi1 and p53 expression in association with DNA strand breaks in idiopathic pulmonary fibrosis. *Am J Respir Crit Care Med* 1996;154:477–483.
36. Plataki M, Koutsopoulos AV, Darivianaki K, Delides G, Siafakas NM, Bouros D. Expression of apoptotic and antiapoptotic markers in epithelial cells in idiopathic pulmonary fibrosis. *Chest* 2005;127:266–274.
37. Wang R, Ramos C, Joshi I, Zagariya A, Pardo A, Selman M, Uhal BD. Human lung myofibroblast-derived inducers of alveolar epithelial apoptosis identified as angiotensin peptides. *Am J Physiol* 1999;277: L1158–L1164.
38. Golan-Gerstl R, Wallach-Dayan SB, Amir G, Breuer R. Epithelial cell apoptosis by fas ligand-positive myofibroblasts in lung fibrosis. *Am J Respir Cell Mol Biol* 2007;36:270–275.
39. Waghray M, Cui Z, Horowitz JC, Subramanian IM, Martinez FJ, Toews GB, Thannickal VJ. Hydrogen peroxide is a diffusible paracrine signal for the induction of epithelial cell death by activated myofibroblasts. *FASEB J* 2005;19:854–856.
40. Adamson IY, Vincent R, Bjarnason SG. Cell injury and interstitial inflammation in rat lung after inhalation of ozone and urban particulates. *Am J Respir Cell Mol Biol* 1999;20:1067–1072.
41. Upadhyay D, Panduri V, Ghio A, Kamp DW. Particulate matter induces alveolar epithelial cell DNA damage and apoptosis: role of free radicals and the mitochondria. *Am J Respir Cell Mol Biol* 2003;29: 180–187.
42. Zheng T, Kang MJ, Crothers K, Zhu Z, Liu W, Lee CG, Rabach LA, Chapman HA, Homer RJ, Aldous D, *et al.* Role of cathepsin S-dependent epithelial cell apoptosis in IFN-gamma-induced alveolar remodeling and pulmonary emphysema. *J Immunol* 2005;174:8106–8115.
43. Yeh WC, Itie A, Elia AJ, Ng M, Shu HB, Wakeham A, Mirtsos C, Suzuki N, Bonnard M, Goeddel DV, *et al.* Requirement for Casper (c-FLIP) in regulation of death receptor-induced apoptosis and embryonic development. *Immunity* 2000;12:633–642.
44. Dohrman A, Russell JQ, Cuenin S, Fortner K, Tschopp J, Budd RC. Cellular FLIP long form augments caspase activity and death of T cells through heterodimerization with and activation of caspase-8. *J Immunol* 2005;175:311–318.
45. Thome M, Tschopp J. Regulation of lymphocyte proliferation and death by FLIP. *Nat Rev Immunol* 2001;1:50–58.
46. Hu WH, Johnson H, Shu HB. Activation of NF-kappaB by FADD, Casper, and caspase-8. *J Biol Chem* 2000;275:10838–10844.
47. Tanaka T, Yoshimi M, Maeyama T, Hagimoto N, Kuwano K, Hara N. Resistance to Fas-mediated apoptosis in human lung fibroblast. *Eur Respir J* 2002;20:359–368.
48. Arsura M, Wu M, Sonenshein GE. TGF beta 1 inhibits NF-kappa B/Rel activity inducing apoptosis of B cells: transcriptional activation of I kappa B alpha. *Immunity* 1996;5:31–40.
49. Mabley JG, Cunningham JM, John N, Di Matteo MA, Green IC. Transforming growth factor beta 1 prevents cytokine-mediated inhibitory effects and induction of nitric oxide synthase in the RINm5F insulin-containing beta-cell line. *J Endocrinol* 1997;155:567–575.
50. Khalil N, O'Connor RN, Unruh HW, Warren PW, Flanders KC, Kemp A, Bereznay OH, Greenberg AH. Increased production and immunohistochemical localization of transforming growth factor-beta in idiopathic pulmonary fibrosis. *Am J Respir Cell Mol Biol* 1991;5: 155–162.
51. Corrin B, Butcher D, McAnulty BJ, Dubois RM, Black CM, Laurent GJ, Harrison NK. Immunohistochemical localization of transforming growth factor-beta 1 in the lungs of patients with systemic sclerosis, cryptogenic fibrosing alveolitis and other lung disorders. *Histopathology* 1994;24:145–150.
52. Clark RAF. Wound repair: overview and general considerations. The molecular and cell biology of wound repair. New York: Plenum Press; 1995. pp. 3–50.
53. Desmouliere A, Redard M, Darby I, Gabbiani G. Apoptosis mediates the decrease in cellularity during the transtion between granulation tissue and scar. *Am J Pathol* 1995;146:56–66.
54. Bruce MC, Honaker CE, Cross RJ. Lung fibroblasts undergo apoptosis following alveolarization. *Am J Respir Cell Mol Biol* 1999;20:228–236.
55. Losa Garcia JE, Rodriguez FM, Martin de Cabo MR, Garcia Salgado MJ, Losada JP, Villaron LG, Lopez AJ, Arellano JL. Evaluation of inflammatory cytokine secretion by human alveolar macrophages. *Mediators Inflamm* 1999;8:43–51.
56. Martinez JA, King TE Jr, Brown K, Jennings CA, Borish L, Mortenson RL, Khan TZ, Bost TW, Riches DW. Increased expression of the interleukin-10 gene by alveolar macrophages in interstitial lung disease. *Am J Physiol* 1997;273:L676–L683.